ACS OMEGA

Open Access

http://pubs.acs.org/journal/acsodf

Article

Novel Acrylate-Based Derivatives: Design, Synthesis, Antiproliferative Screening, and Docking Study as Potential Combretastatin Analogues

Eman Fayad, Sarah Awwadh Altalhi, Matokah M. Abualnaja, Abdulmohsen H. Alrohaimi, Fahmy G. Elsaid, Ali H. Abu Almaaty, Rasha Mohammed Saleem, Mohammed A. Bazuhair, Ali Hassan Ahmed Maghrabi, Botros Y. Beshay, and Islam Zaki*

Cite This: *ACS Omega* 2023, 8, 38394−38405

Read Online

ACCESS | Metrics & More | Article Recommendations | Supporting Information

ABSTRACT: A variety of 3-(4-chlorophenyl) acrylic acids **4a,b** and 3-(4-chlorophenyl)acrylate esters **5a−i** were synthesized and structurally proven by spectroscopic studies such as IR, ^{1}H NMR, and ^{13}C NMR as well as mass spectrometry. All substances were investigated for their antiproliferative efficacy against the MDA-MB-231 cell line. Among these, acrylic acid compound **4b** demonstrated the most potent cytotoxic effect with an IC_{50} value of 3.24 ± 0.13 μM, as compared to CA-4 (IC_{50} = 1.27 ± 09 μM). Additionally, acrylic acid molecule **4b** displayed an inhibitory effect against β-tubulin polymerization with a percentage inhibition of 80.07%. Furthermore, compound **4b** was found to produce considerable cell cycle arrest at the G2/M stage and cellular death, as demonstrated by FACS analysis. In addition, the in vivo antitumor screening of the sodium salt of acrylic acid **4b** was carried out, and the results have shown that the tested molecule showed a significant decrease in viable EAC count and EAC volume, accompanied by a considerable increase in the life span prolongation, if compared to the positive control group. Furthermore, molecular modeling studies were performed to understand how the highly efficient chemicals **4b** and **5e** interact with the colchicine-binding region on tubulin. This work aims to shed light on the reasons behind their exceptional cytotoxicity and their better capacity to inhibit tubulin in comparison to CA-4.

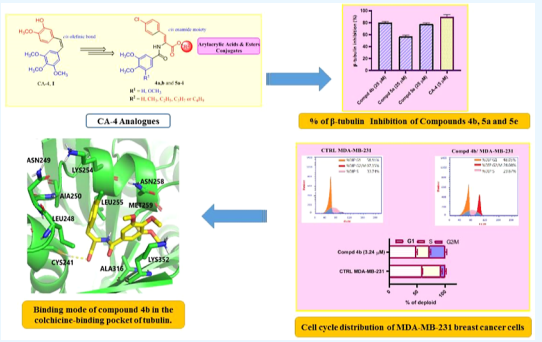

1. INTRODUCTION

One of the leading causes of death worldwide is cancer.[1] Despite the availability of different chemotherapeutic agents, no effective regimens for dealing with cancer sequences have been proposed, and the disease remains lethal and terrible.[2,3] Microtubules, including α- and β-tubulin subunits, play a critical role in numerous biological activities, including spindle formation and cellular shape maintenance.[4,5] In order to prepare the chromosomes for cell division into a pair of daughter cells, tubulin is polymerized during the cellular cycle to form microtubules.[6,7] Microtubules are an attractive target for the development of anticancer drugs due to their function in cell mitosis.[8,9] The usual tubulin inhibitor, combretastatin A-4 (CA-4) I, binds to the colchicine (Col) site, causing microtubule depolymerization and the apoptotic death of cancer cells.[10,11] For the synthesis of related compounds that may have future biological functions, CA-4 I has acted as a fundamental structural template.[12] Numerous compounds that resemble CA-4 have been created and studied as possible anticancer drugs.[13−15] Two aromatic rings are connected by a different moiety, such as olefins, enamides, or heterocyclic functions, to form CA-4 analogues.[16−18] According to SAR studies, ring A's trimethoxy group is a crucial pharmacophoric site for tubulin, whereas ring B's halogenated phenyl group preserves the antitubulin activity.[19,20] The maintenance of tissue growth and homeostasis depends heavily on apoptosis, a critical cellular function.[21,22] Apoptotic pathway regulation issues have been connected to a variety of diseases, including cancer.[23] In order to find effective cancer treatments, it has become common practice to design and prepare novel chemotherapeutic chemicals that are capable of triggering apoptotic death.[24−26]

Much emphasis has been paid to the construction of scaffolds with tiny molecular structures as their principal structural design in the hunt for potential anticancer candidates.[15,27] The acrylate moiety, a synthetic small molecular scaffold, is a prized element in modern medical

Received: July 13, 2023
Accepted: September 22, 2023
Published: October 9, 2023

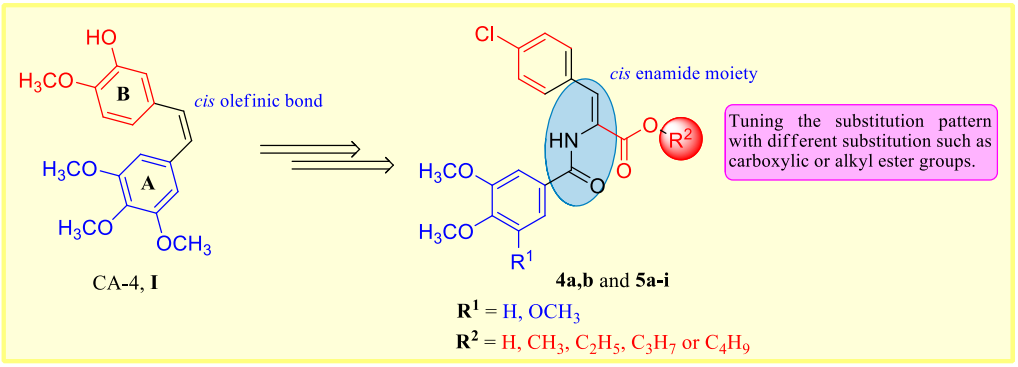

Figure 1. Molecular structure design of the synthesized acrylate derivatives **4a,b** and **5a−i**.

Scheme 1. Synthesis of Target Acrylate Compounds 4a,b, and 5a−i[a]

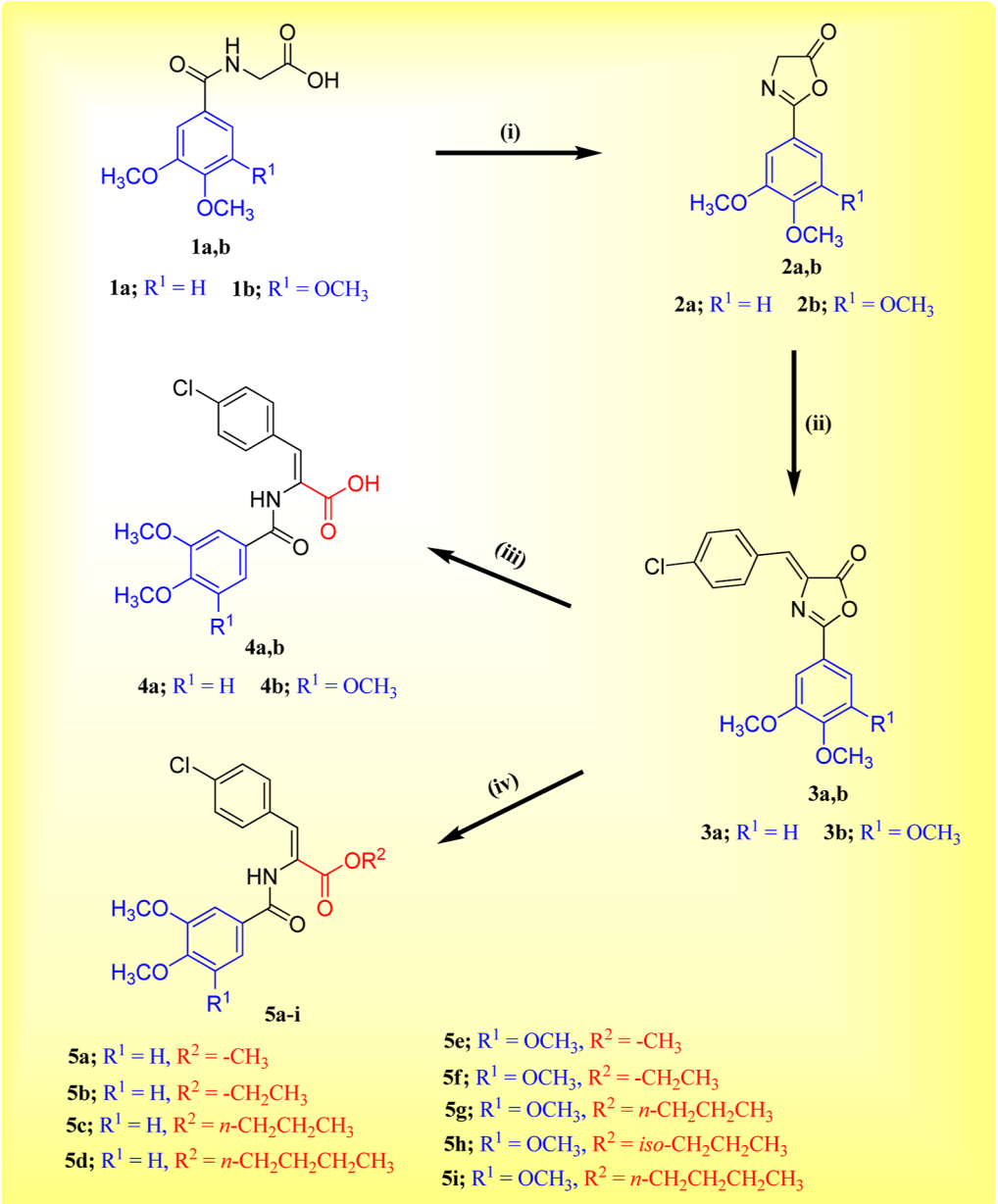

[a]Reagents: (i) Ac_2O at 70 °C for 40 min; (ii) 4-chlorobenzaldehyde in NaOAc reflux for 2 h; (iii) 20% KOH reflux for 1−2 h; (iv) appropriate aliphatic alcohol in NaOAc reflux for 5−6 h.

https://doi.org/10.1021/acsomega.3c05051
ACS Omega 2023, 8, 38394−38405

chemistry.[28] The molecules based on this scaffold have a wide range of actions, such as anticancer, antioxidant, and anti-inflammatory medicines, due to their broad scope and affinity for a number of biological targets.[29−31]

As potential chemotherapeutic agents, compounds containing acrylate groups play a crucial role in inducing apoptotic cell death and disrupting tubulin polymerization, thereby exerting their anticancer effects.[32,33] Specifically, structurally akin to chalcone and aroylacrylic acids, the substituted benzoylacrylic acids demonstrate a capacity to inhibit EGFR selectively and covalently, as elucidated in a previous study.[32] Furthermore, a study by Hao et al.[33] has highlighted the ability of acrylic phenethyl ester-2-pyranone derivatives to induce apoptosis and G2/M cell cycle arrest by targeting GRP94 in colorectal cancer. Additionally, the indole-3-acrylic acid conjugates demonstrated exceptionally potent anticancer agents that exhibit effectiveness against a diverse range of hematological and solid human tumor cell lines.[34]

In light of these findings, our primary objective is to design and synthesize novel aryl acrylic acids (**4a,b**) and acrylate esters (**5a−i**) integrated into the trimethoxybenzene scaffold of CA-4, connected via a carboxamide linker (Figure 1). The intention behind this design is to explore the potential antiproliferative effects of these compounds on the MDA-MB-231 breast cancer cell line. To comprehensively understand the mechanisms at play, our investigation will encompass cellular mechanistic studies. This will encompass evaluating the compounds' capacity to induce apoptosis, impact tubulin polymerization, and trigger cell cycle arrest. Furthermore, molecular modeling studies are undertaken to elucidate the underlying basis for the potent antiproliferative activities observed in the most active candidates.

2. RESULTS AND DISCUSSION

2.1. Chemistry. Scheme 1 depicts a general schematic of the synthesis of the target substances 3-(4-chlorophenyl)acrylic acids **4a,b** and 3-(4-chlorophenyl)acrylate esters **5a−i**. The crucial oxazolone intermediate **3a,b** was produced by cyclo-condensing 4-chlorobenzaldehyde with the active methylene molecule, 2-aryl-2-oxazoline-5-one. As a representative example, the infrared (IR) spectra of compound **3b** revealed a prominent stretching band at 1801 cm^{-1}, which corresponded to the lactone ring's C═O.

The required 3-(4-chlorophenyl)acrylic acids **4a,b** were produced by reacting the important oxazolone intermediates **3a,b** with 20% KOH. The acrylic acid derivative **4b** could be easily deduced since there were two clear broad signals of carboxylic−OH and amidic−NH protons at δ 12.85 and 9.91 ppm, respectively. In addition, the two aromatic protons of the 3,4,5-trimethoxyphenyl (TMP) moiety of compound **4b** appeared as a singlet signal at δ 7.33 ppm. Additionally, the 4-chlorophenyl protons of compound **4b** appeared as two doublet of doublet signals at δ 7.67 and 7.48 ppm with integral two protons for each signal. The aliphatic methoxy protons of compound **4b** were observed as two set signals at δ 3.85 and 3.74 ppm, integrating six and three protons, respectively. The close examination of the ^{13}C nuclear magnetic resonance (NMR) spectrum of acrylic acid derivative **4b** revealed two carbonyl groups (C═O) at δ 166.67 and 165.77 ppm assigned to carboxylic acid and amidic groups, respectively. All the aromatic and aliphatic carbons of compound **4b** were found in the ranges of δ 153.16−105.80 and 60.57−56.53 ppm, respectively. The ^{1}H NMR spectra of compound **4a**, an acrylic acid, were discovered to follow a pattern identical to that of compound **4b**.

The 3-(4-chlorophenyl)acrylate ester derivatives **5a−i** were produced by heating **3a,b** at reflux with appropriate aliphatic alcohols, including methyl alcohol, ethyl alcohol, n-propyl alcohol, isopropyl alcohol, and *n*-butyl alcohol, while also being in the presence of anhydrous sodium acetate (NaOAc). Compounds **5a−i** had a common singlet signal due to the −NH group of the amide moiety at δ 10.08−9.93 ppm in the ^{1}H-NMR spectra of the title molecules. Additionally, doublets of doublet signals at ppm δ 7.70−7.67 and 7.50−7.47 that were attributable to the 4-chlorophenyl group shared two characteristic signals. Additionally, the aliphatic and olefinic protons showed up at the predicted chemical shifts. The carbonyl carbon (C═O) of the acrylate ester moiety can be found at δ 166.04−165.47 ppm in the ^{13}C NMR spectra of the 3-(4-chlorophenyl)acrylate ester derivatives **5a−i**, while the carbonyl carbon (C═O) of the amide function can be found at δ 165.85−164.78 ppm. Additionally, the compounds **5a−i's** ^{13}C NMR spectra revealed unique methoxy carbons in the range of δ 60.57−52.30 ppm. At the anticipated chemical shift signals, the aliphatic, olefinic, and aromatic carbons were visible. The newly produced acrylate compounds 4a, b, and **5a−i** were also found to be pure, and elemental studies confirmed this, with the results correlating with the products' chemical formula.

2.2. Biology. *2.2.1. In Vitro Cytotoxic Activity against MDA-MB-231 Breast Carcinoma Cell Line.* 3-(4-Chlorophenyl)acrylic acids **4a,b** and 3-(4-chlorophenyl)-acrylate esters **5a−i** were recently synthesized compounds whose cytotoxic activity was evaluated using the MTT method against the MDA-MB-231 human breast carcinoma cell line. Cytotoxic activity against the breast cancer cell line MDA-MB-231 in vitro Table 1, outlines the results, and provides them as

Table 1. IC_{50} (μM) Values of the Prepared Molecules against MDA-MB-231 Cancerous Cells[a]

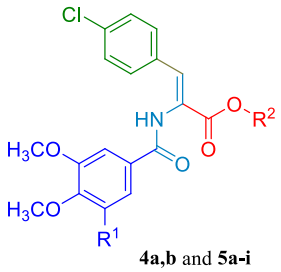

4a,b and **5a-i**

comp no	R^1	R^2	IC_{50} value (μM) MDA-MB-231	IC_{50} value (μM) MCF-10A
4a	H	H	8.24 ± 0.37	NT
4b	OCH_3	H	3.24 ± 0.13	23.29 ± 0.32
5a	H	CH_3	4.84 ± 0.19	NT
5b	H	C_2H_5	15.81 ± 0.41	NT
5c	H	*n*-C_3H_7	14.26 ± 0.33	NT
5d	H	*n*-C_4H_9	45.86 ± 1.02	NT
5e	OCH_3	CH_3	4.03 ± 0.16	NT
5f	OCH_3	C_2H_5	11.59 ± 0.24	NT
5g	OCH_3	*n*-C_3H_7	23.21 ± 0.40	NT
5h	OCH_3	*iso*-C_3H_7	25.25 ± 0.51	NT
5i	OCH_3	*n*-C_4H_9	28.11 ± 0.56	NT
CA-4			1.27 ± 09	14.21 ± 0.29

[a]NT; not tested.

https://doi.org/10.1021/acsomega.3c05051
ACS Omega 2023, 8, 38394−38405

IC_{50} values, using Col as the positive control. The examined acrylate compounds have variable degrees of cytotoxicity when applied to the MDA-MB-231 cell line. Compounds **4b, 5a**, and **5e** were the most effective acrylate molecules on cell viability and caused inhibition of cell proliferation with IC_{50} ranges from 3.24 to 4.83 M, followed by compounds **4a, 5b, 5c**, and **5f** with IC_{50} values ranges from 8.55 to 15.89 M. The activity of the newly synthesized molecules can be arranged in descending order as follows. However, the IC_{50} values for the acrylate ester compounds **5g, 5h**, and **5i** were higher, ranging from 23.15 to 28.06 M. The least active substance was compound **5d**, with an IC_{50} value of 45.78 M. Additionally, it was shown that, when compared to CA-4 (IC_{50} = 1.27 M), acrylic acid derivative **4b** (IC_{50} = 3.24 M) was the most effective anticancer drug against MDA-MB-231 breast carcinoma cells, followed by methyl acrylate compound **5e** (IC_{50} = 4.06 M). It is therefore reasonable to believe that the anticancer activity of the 3-(4-chlorophenyl) acrylate derivatives **4a,b**, and **5a−i** against MDA-MB-231 cells predominated over the presence of a carboxylate or methylate moiety. Finally, the cytotoxic action was reduced when the TMP ring was replaced with a dimethoxyphenyl group, showing that the TMP is more tolerable for the antiproliferative activity. It is noteworthy that the synthesized acrylic acid derivative **4b** revealed a higher IC_{50} to normal MCF-10A breast cells; IC_{50} = 23.29 μM (Table 1). The mean tumor selectivity index calculated for compound **4b** was found to be 7.2, which demonstrates good selectivity toward tumor cells.

2.2.2. β-Tubulin Polymerization Inhibition Activity. Previous reports suggested that β-tubulin polymerization is a multistep process triggered by the creation of assembled protofilaments as well as the regulation of actin filaments.[35] As a crucial component of the cytoskeleton, β-tubulin polymerization has been identified as a possible target in cancer drug development.[36] To evaluate whether the representative active acrylate derivatives target the tubulin-microtubule system, compounds **4b**, **5a,** and **5e** were selected to investigate their abilities to disrupt microtubule assembly. The impact of selected newly prepared acrylate derivatives **4b**, **5a,** and **5e** on β-tubulin polymerization at a concentration value of 25 μM is outlined in Figure 2. CA-4 was included as a reference compound. The results demonstrated that compounds **4b** and **5e** were proven to be strong inhibitors with β-tubulin polymerization inhibition activity percentages of 80.07 and 77.81%, respectively, comparable to CA-4 (inhibition value of 89.77%). It is clear from the results that tubulin was the molecular target of these compounds and that this molecular target interferes with microtubule polymerization. Treatment with compound **5a** at a concentration of 25 M, on the other hand, prevented the polymerization of tubulin by 57.13%.

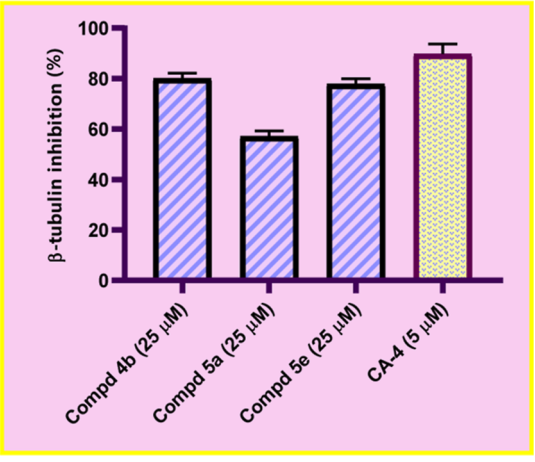

Figure 2. Effect of compounds **4b**, **5a,** and **5e** on β-tubulin polymerization was investigated using an ELISA assay for β-tubulin. Results are the averages of three tests with n = 3 and CA-4 as the reference molecule.

2.2.3. Cell Cycle Analysis. Chemotherapy for cancer may target cells in the G2M stage of the cell cycle.[37] Numerous studies have demonstrated that tubulin assembly inhibitors can stop cancer cells in the G2/M stage and induce cellular apoptosis.[38] We used a flow cytometric assay to further assess the cellular molecular mechanism activities of 3-(4-chlorophenyl) acrylic acid **4b** in MDA-MB-231 malignant cells due to its strong ability to block -tubulin polymerization. The effect of acrylic acid derivative **4b** on the advancement of the cell cycle in MDA-MB-231 cells was investigated in order to validate the cellular mechanism. As demonstrated in Figure 3, untreated control MDA-MB-231 cells had a typical cell cycle pattern at each stage, including the G1, S, and G2M phases. In contrast, cancer cell accumulation was found at the G2/M stage to be 3.82 times higher in the treated group of MDA-MB-231 cells than in the untreated control group after treatment with acrylic acid derivative **4b** at a concentration equivalent to its IC_{50} value (3.24 M). It is important to note that the percentage of G2M phase increased from 7.35% in the control group to 28.08% in the acrylic acid **4b**-treated group. The findings demonstrate that acrylic acid **4b** can prevent cell mitosis and stop MDA-MB-231 cells in the G2M phase, which reduces MDA-MB-231 cellular growth and proliferation.

2.2.4. Cell Apoptosis Analysis. An Annexin V-FITCPI (AVPI) double staining technique was used to assess compound **4b's** ability to trigger apoptosis in order to ascertain whether it might do so. MDA-MB-231 cells were stained with two dyes and subjected to a FACS analysis after 48 h of treatment with acrylic acid **4b** at its IC_{50} dose (3.24 M). It was discovered that acrylic acid **4b** might accelerate late-secondary cellular apoptosis, increasing it from 0.24% in the control untreated group to 12.62% in the acrylic acid **4b** treated group (Figure 4). Additionally, a rise in early primary apoptosis was observed, going from 0.69% in the control group that received no treatment to 8.09% in the cells that were treated with acrylic acid **4b** (Figure 4). According to these results, this class of chemicals may harm MDA-MB-231 cells while they are in the G2/M phase and cause apoptosis.

2.2.5. In Vivo Antitumor Screening. The in vivo antitumor activity of acrylic acid derivative **4b** against EAC cells mice was evaluated by parameters such as EAC counting, EAC volume, and life span prolongation. For the in vivo studies, the acrylic acid derivative **4b** was converted into sodium salt to enhance its bioavailability. The highest efficacious dose of the acrylic acid derivative **4b** was found to be 20 mg/kg, as evidenced by the intraperitoneal injection of the EAC carrying mice with various concentrations of the sodium salt of compound **4b**. Figure 5A shows how many EAC cells there were in the study group. The findings showed that after treatment with 20 mg/kg of the sodium salt of compound **4b**, the mean number of EAC cells in EAC-bearing mice fell from 358.47×10^6 to 39.12×10^6. Similar to this, it was discovered that the mean EAC cell volume in EAC-bearing mice was 5.720.71. For the group that received the sodium salt of component **4b**, it was 0.370.19

https://doi.org/10.1021/acsomega.3c05051
ACS Omega 2023, 8, 38394−38405

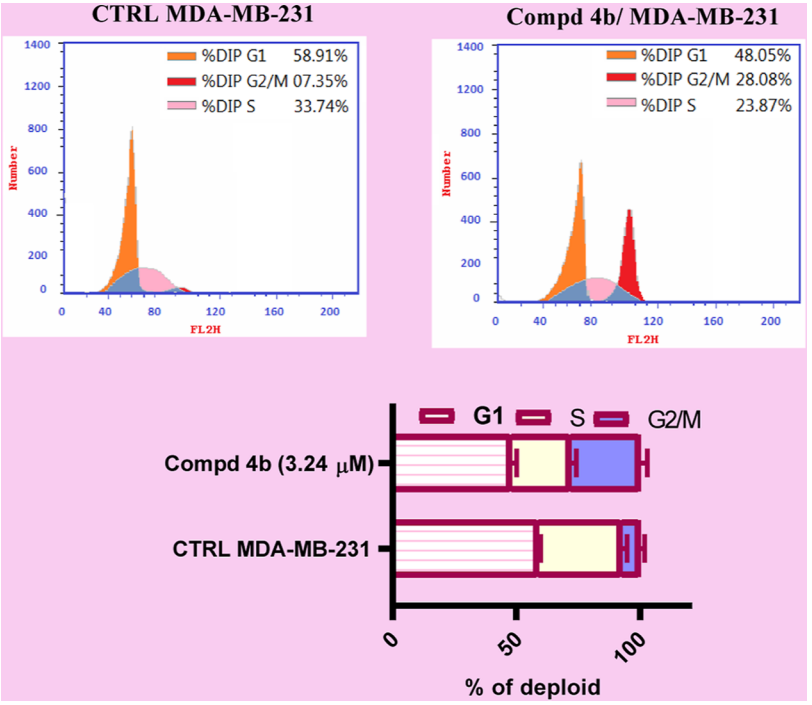

Figure 3. Cell cycle distribution of MDA-MB-231 breast cancer cells after 48 h of treatment with compound **4b**.

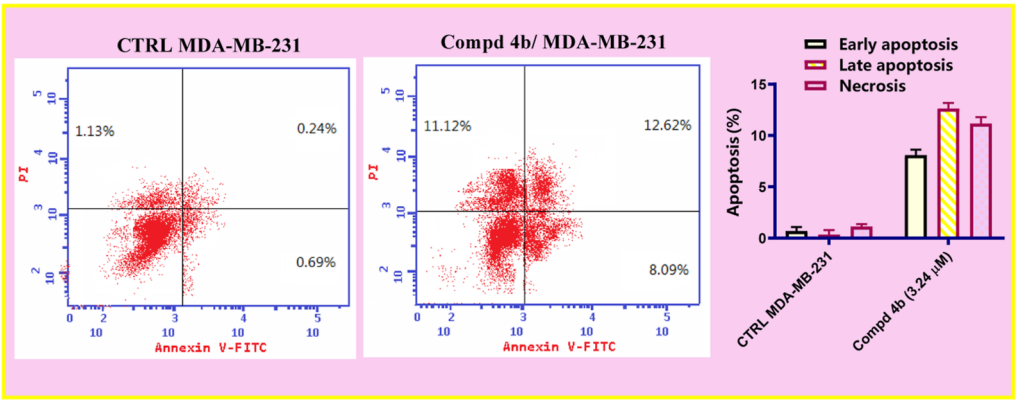

Figure 4. Annexin V-FITC/propidium iodide assay method. MDA-MB-231 cells were treated with acrylic acid compound **4b** for 48 h and stained with Annexin V-FITC and/or propidium iodide and counted for apoptosis using a flow cytometer.

(Figure 5B). When compared to the positive control group, the EAC volume in the mice treated with the sodium salt of chemical **4b** dramatically decreased by 15.46-fold. Additionally, Figure 5C showed how compound **4b's** sodium salt affected the study group's life expectancy. The outcomes showed that the mice treated with sodium salt of compound 4b had a life expectancy extension of (41) days as opposed to the control group's (16) days. When compared to the EAC cell positive group, it was discovered that the control group treated with sodium salt of chemical **4b** had a 2.56-fold longer life expectancy. The findings of the current investigation unquestionably demonstrate the sodium salt of the acrylic acid derivative **4b's** tumor-inhibitory efficacy against EAC cells. According to our findings, sodium acrylate **4b** treatment had a substantial impact on the EAC cell count and EAC volume of ascites tumor-bearing animals. This was accompanied by an increase in the life expectancy in the treated group. These results unmistakably demonstrate the antitumor activity of compound **4b** of acrylic acid against EAC.

2.2.6. Molecular Docking Study. The exceptional cytotoxicity and tubulin inhibitory activity displayed by the very powerful compounds **4b** and **5e** compared to CA-4 were interestingly revealed by molecular docking research. Notably, with binding free energies of −6.1, −6.7, and −6.4 kcal/mol, respectively, all three compounds, CA-4, **4b**, and **5e**, were discovered to exactly fit and occupy the desired Col binding position on tubulin (Figure 6). The important amino acid residue Cys241 was found to form hydrogen bonds with both CA-4 and compound **4b** (Figure 8), according to closer inspection (Figures 7−9), while compound **5e** (Figure 9) established a strong hydrophobic interaction and S-halogen interaction with the conserved amino acid (Cys241). Additionally, a number of amino acids, including Gln247, Leu248, Ala250, Lys254, Leu255, Asn258, Lys352, and Ala316, had strong hydrophobic interactions that provided a thorough description of the tubulin pocket.

The important hydrogen connection produced by the carboxylate functionality with Cys241 and the strong hydro-

https://doi.org/10.1021/acsomega.3c05051
ACS Omega 2023, 8, 38394−38405

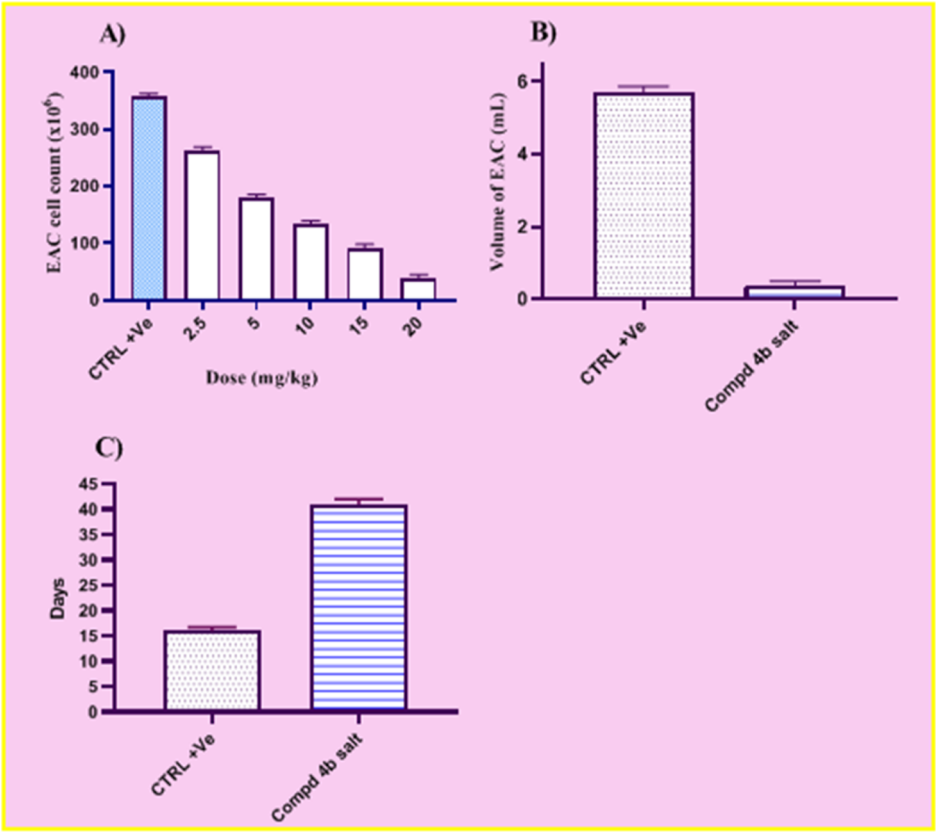

Figure 5. Impact of sodium salt of compound **4b** on tumor size parameters of EAC-bearing mice (A) EAC cell count at different doses (mg/kg); (B) EAC volume; (C) life span prolongation. Data expressed as the mean ± SE (n = 10).

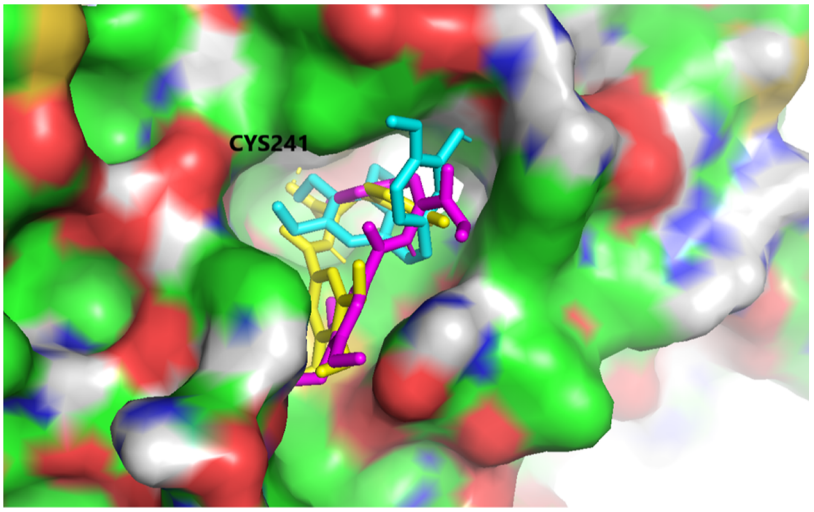

Figure 6. Superposition of CA-4 (cyan), 4b (yellow), and 5e (magenta) in the Col-binding pocket of tubulin in surface view depiction. The hydrogen bond with the key amino acid residue Cys241 is shown to be conserved in CA-4 and its analogues **4b** and **5e**.

phobic contacts between the chlorophenyl fragment of **4b** and the hydrophobic groove formed by Leu248, Ala250, Lys254, and Leu255 are both responsible for the enhanced inhibitory binding activity of **4b**. It is interesting to note that the provital H-bond with Cys241 was broken by esterification of the carboxylate functionality in **5e**. This could account for **5e**′**s** slightly lower tubulin-binding inhibitory efficacy than **4b**. It is noteworthy that the polar interactions with Leu248, Met259, and Lys254 as well as the hydrophobic interactions involving the side chains of the aforementioned amino acid residues, as well as the hydrogen bond and hydrophobic interaction with Cys241, played a significant role in the intricate process of protein−ligand binding. These important interactions probably play a role in the exceptional tubulin inhibitory activity that CA-4, compounds **4b**, and compound **5e** all exhibit.[39−41] The results of the docking study point to compounds **4b** and **5e**′**s** extraordinary capacity to disrupt the process of tubulin polymerization as the likely cause of their potent cytotoxic effects on the MDA-MB-231 breast cancer cell line.

https://doi.org/10.1021/acsomega.3c05051
ACS Omega 2023, 8, 38394−38405

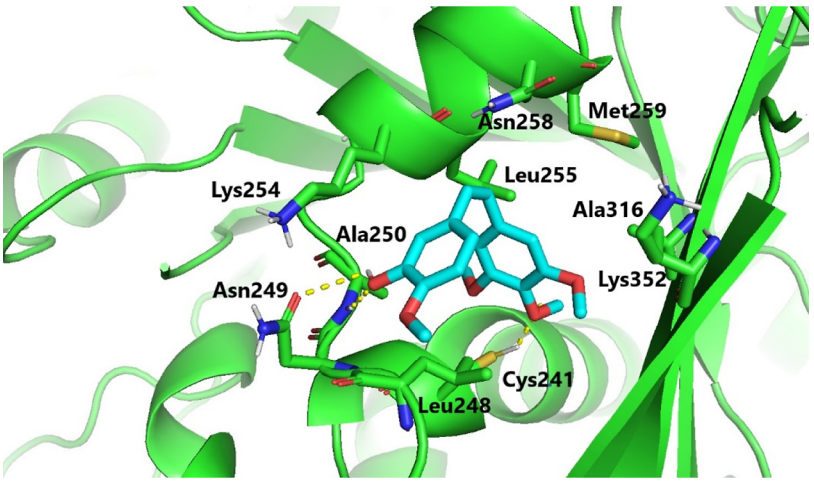

Figure 7. Binding mode of CA-4 in the Col-binding pocket of tubulin. Hydrogen bonds are shown by yellow dashed lines.

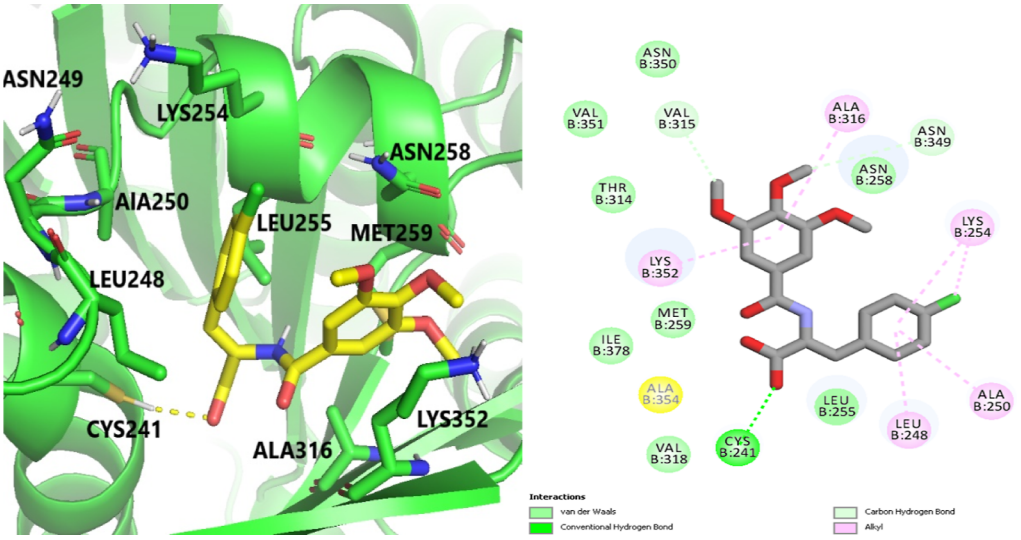

Figure 8. Binding mode of compound **4b** (3D left panel and 2D right panel) in the Col-binding pocket of tubulin. Hydrogen bonds are shown by yellow dashed lines.

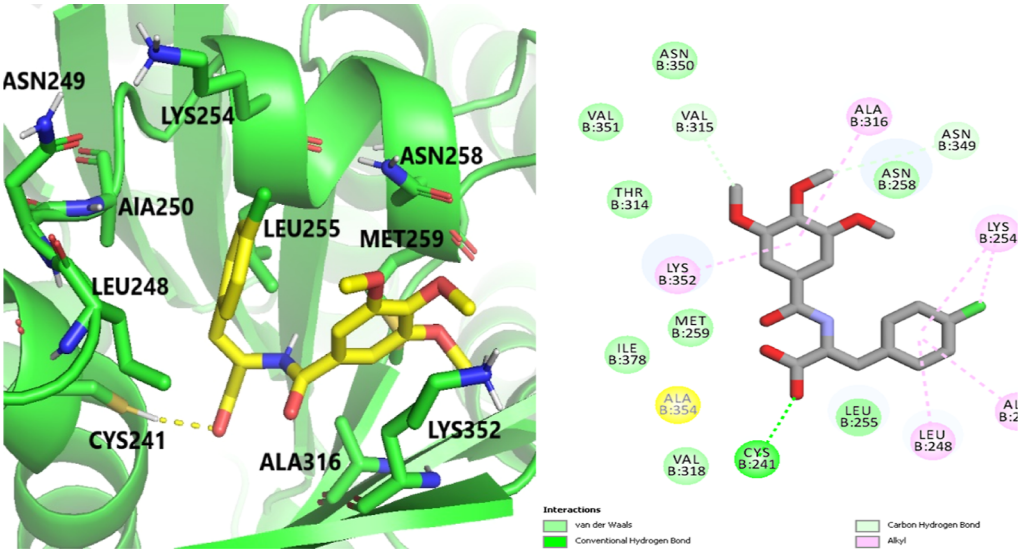

Figure 9. Binding mode of compound **5e** (3D left panel and 2D right panel) in the Col-binding pocket of tubulin. Hydrogen bonds are shown by yellow dashed lines.

https://doi.org/10.1021/acsomega.3c05051
ACS Omega 2023, 8, 38394−38405

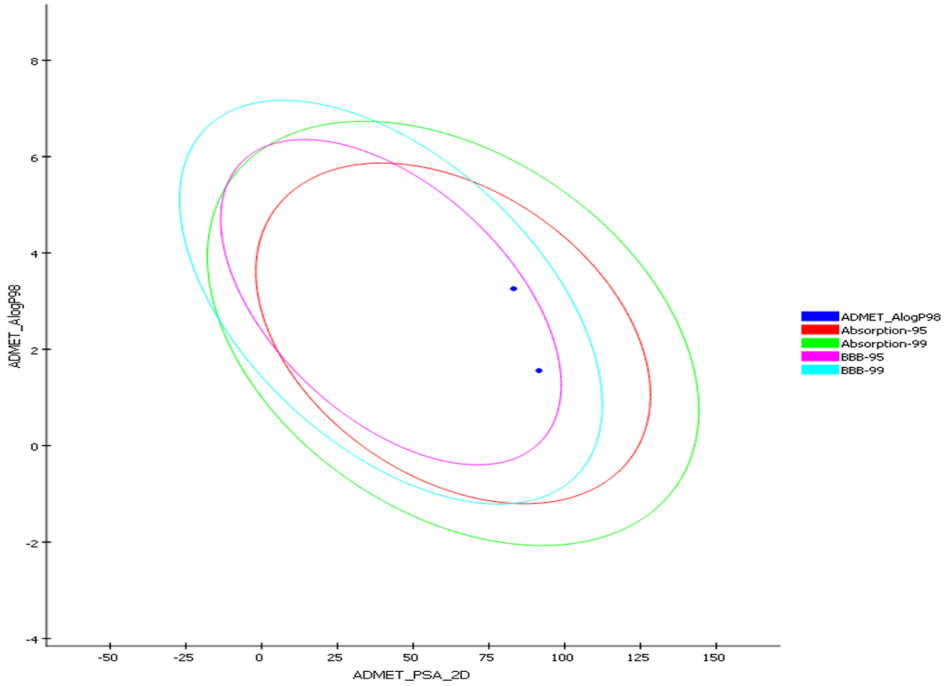

Figure 10. For acrylate molecules **4b** and **5e**, the HIA and blood brain barrier plots are shown.

*2.2.7. In Silico Predictive ADME Study for Targeted Compounds **4b** and **5e**.* Using the Discovery Studio suite v.5,[42] computer-assisted absorption-distribution-metabolism-elimination-and-toxicity (ADMET) tests were carried out to evaluate the pharmacokinetic properties of **4b** and **5e**, which showed strong activity. The water solubility, absorption, atom-based Log P98, two-dimensional (2D) polar surface area, blood−brain barrier (BBB) level, and likelihood of cytochrome P450 2D6 activity were all factors that this research looked at in relation to the chemical structure of compounds **4b** and **5e**. The analysis of the PSA_2D and A LogP98 characteristics produced the data shown in the ADMET plot (Figure 10), which offered important details about the pharmacokinetics of the drugs. Additionally, the ability of **4b** and **5e** to be absorbed and permeate the brain was assessed by looking at the human intestinal absorption (HIA) and BBB plots. Compounds **4b** and **5e** have limited ability to passively cross the BBB, which could result in adverse effects on the central nervous system, according to the dots on the BBB plot (Figure 10). Figure 10's depiction of the HIA plot revealed that **4b** and **5e** had good intestinal absorption, with a sizable proportion of the drug able to passively cross the intestine, as opposed to the BBB. Furthermore, the chemical showed good water solubility. Compounds **4b** and **5e** were discovered to have good bioavailability overall based on the ADMET characteristics (**4b** PSA = 91.51 and **5e** PSA = 83.132), whereas molecules with PSA >140 tend to have poor bioavailability. Table 2 contains comprehensive computations of the ADMET parameters.

Table 2. Computer-Aided ADMET Parameters of Acrylate Compounds 4b and 5e

parameter	4b	5e
BBB_Lev[a]	3	2
absorption Lev[b]	0	0
AQ SOL Lev[c]	3	2
Alog P98[d]	1.55	3.25
ADME_PSA_lev	91.51	83.132

[a]Blood brain barrier level; 4 = undefined, 3 = low penetration, 2 = medium penetration, 1 = high penetration. [b]Absorption Level; 3 = very low absorption, 2 = low absorption, 1 = moderate, 0 = good absorption. [c]Aqueous solubility level; 4 = optimal, 3 = good, 2 = low solubility, 1 = very low but soluble, 0 = extremely low. [d]Polar surface area; compounds must have a log p value not greater than 5.0 to attain reasonable probability of being well absorbed.

3. CONCLUSIONS

In summary, the intermediate oxazolone derivatives **3a,b** were used to manufacture the target compounds, 3-(4-chlorophenyl)acrylic acids **4a,b**, and 3-(4-chlorophenyl)-acrylate esters **5a−i**. Spectroscopic methods confirmed the chemical structures of the generated compounds. The MDA-MB-231 breast cells were tested for in vitro cytotoxic activities against the target acrylate derivatives. The most effective compound against MDA-MB-231 breast cancer cells was discovered to be acrylic acid derivative **4b**, with an IC_{50} value of 3.24 M as opposed to CA-4 (IC_{50} = 1.27 M). In comparison to CA-4 (inhibition percentage 89.77%), acrylic acid compound **4b** showed good tubulin polymerization inhibition effectiveness with a percent inhibition value of 80.07%. Additionally, in cellular mechanistic investigations, it was discovered that the representative acrylic acid derivative **4b** caused significant cell cycle stopping at the G2/M phase and cellular death in MDA-MB-231 cells. The sodium salt of compound **4b's** in vivo anticancer testing had a significant impact on lowering the EAC count and tumor volume. In addition, it boosted the life expectancy extension in comparison to the favorable control group. Furthermore, according to the docking results, the exceptional cytotoxicity of compounds **4b** and **5e** against the MDA-MB-231 cells may be caused by their strong inhibition of tubulin polymerization.

https://doi.org/10.1021/acsomega.3c05051
ACS Omega 2023, 8, 38394−38405

4. EXPERIMENTAL SECTION

4.1. Chemistry. *4.1.1. General.* General details in Supporting Information Appendix A

*4.1.2. General Process for Synthesizing (Z)-3-(4-Chlorophenyl)-2-(substitutedbenzamido)acrylic Acids **4a,b**.* For 1−2 h, a suspension of oxazolone derivative **3a,b** (0.01 mol) in potassium hydroxide (20%, 25 mL) was refluxed. Following the completion of the reaction, the reaction mixture was cooled and neutralized with a weak hydrochloric acid. The precipitated product was crystallized with aqueous ethanol (70%) to afford pure acrylic acid compound **4a,b**.

*4.1.2.1. (Z)-3-(4-Chlorophenyl)-2-(3,4-dimethoxybenzamido)acrylic Acid (**4a**).* Yield (1.37 g, 38%) mp 211−213 °C. IR (ATR, ν, cm^{-1}): 3112−2610 (br OH), 3192 (NH), 2935, 2867 (CH aliphatic), 1682, 1630 (C═O), 1586, 1504 (C═C), 1298, 1205 (C−O). ^{1}H NMR (400 MHz, DMSO-d_6) (δ, ppm): 12.84 (*s*, 1H, O−H), 9.79 (*s*, 1H, N−H), 7.62 (*dd*, *J* = 25.5, 10.0 Hz, 2H, Ar−H), 7.53 (*d*, *J* = 10.2 Hz, 1H, Ar−H), 7.48−7.40 (*m*, 2H, Ar−H), 7.38 (*d*, *J* = 6.0 Hz, 1H, Ar−H), 7.36 (*s*, 1H, olefinic CH), 7.08 (*d*, *J* = 8.3 Hz, 1H, Ar−H), 3.83 (*s*, 3H, OCH_3), 3.81 (*s*, 3H, OCH_3). MS (*m*/*z*, %): 361.07 (M^+, 24.62), 208.23 (100). Found: C, 59.83; H, 4.54; N, 3.81; $C_{18}H_{16}ClNO_5$ (361.78) requires C, 59.76; H, 4.46; N, 3.87.

*4.1.2.2. (Z)-3-(4-Chlorophenyl)-2-(3,4,5-trimethoxybenzamido)acrylic Acid (**4b**).* Yield (1.80 g, 46%) mp 227−229 °C. IR (ATR, ν, cm^{-1}): 3115−2612 (br OH), 3193 (NH), 2935, 2867 (CH aliphatic), 1682, 1630 (C═O), 1586, 1504 (C═C), 1298, 1152 (C−O). ^{1}H NMR (400 MHz, DMSO-d_6) (δ, ppm): 12.85 (*s*, 1H, O−H), 9.91 (*s*, 1H, N−H), 7.67 (*d*, *J* = 8.6 Hz, 2H, Ar−H), 7.48 (*d*, *J* = 8.6 Hz, 2H, Ar−H), 7.41 (*s*, 1H, olefinic CH), 7.33 (*s*, 2H, Ar−H), 3.85 (*s*, 6H, $2OCH_3$), 3.74 (*s*, 3H, OCH_3). ^{13}C NMR (100 MHz, DMSO-d_6) (δ, ppm): 166.67, 165.77, 153.16, 140.99, 134.19, 133.18, 131.86, 131.42, 129.15, 128.85, 128.58, 105.80, 60.57, 56.53. MS (*m*/*z*, %): 391.55 (M^+, 38.02), 206.24 (100). Found: C, 58.16; H, 4.69; N, 3.64; $C_{19}H_{18}ClNO_6$ (391.80) requires C, 58.24; H, 4.63; N, 3.57.

*4.1.3. General Process for Synthesizing (Z)-3-(4-Chlorophenyl)-2-(substitutedbenzamido)acrylate Esters **5a−i**.* A mixture of oxazolone derivative **3a,b** (0.01 mol), appropriate primary alcohol (25 mL), and anhydrous NaOAc (1.48 g, 0.018 mol) was heated to reflux for 5−6 h. The mixture was chilled before being placed into 50 mL of ice-cold water. To get pure acrylate ester derivatives **5a−i**, the precipitate was purified by column chromatography with chloroform: methanol (9:1) as eluent.

*4.1.3.1. (Z)-Methyl 3-(4-Chlorophenyl)-2-(3,4-dimethoxybenzamido)acrylate (**5a**).* Yield (2.03 g, 54%) mp 141−143 °C. IR (ATR, ν, cm^{-1}): 3322 (NH), 3018 (CH aromatic), 2969, 2878 (CH aliphatic), 1714, 1648 (C═O), 1587, 1505 (C═C), 1249, 1186 (C−O). ^{1}H NMR (400 MHz, DMSO-d_6) (δ, ppm): 9.96 (*s*, 1H, N−H), 7.67 (*d*, *J* = 8.5 Hz, 2H, Ar−H), 7.63 (*d*, *J* = 8.4 Hz, 1H, Ar−H), 7.54 (*s*, 1H, Ar−H), 7.47 (*d*, *J* = 8.5 Hz, 2H, Ar−H), 7.35 (*s*, 1H, olefinic CH), 7.08 (*d*, *J* = 8.4 Hz, 1H, Ar−H), 3.84 (*s*, 3H, OCH_3), 3.82 (*s*, 3H, OCH_3), 3.73 (*s*, 3H, OCH_3). ^{13}C NMR (100 MHz, DMSO-d_6) (δ, ppm): 165.61, 165.52, 151.97, 148.41, 133.89, 132.51, 131.46, 130.93, 128.70, 127.52, 125.27, 121.30, 111.04, 110.98, 55.69, 55.59, 52.30. MS (*m*/*z*, %): 375.13 (M^+, 18.36), 296.10 (100). Found: C, 60.83; H, 5.02; N, 3.62; $C_{19}H_{18}ClNO_5$ (375.80) requires C, 60.72; H, 4.83; N, 3.73.

*4.1.3.2. (Z)-Ethyl 3-(4-Chlorophenyl)-2-(3,4-dimethoxybenzamido)acrylate (**5b**).* Yield (1.99 g, 51%) mp 163−165 °C. IR (ATR, ν, cm^{-1}): 3303 (NH), 3018 (CH aromatic), 2978, 2874 (CH aliphatic), 1712, 1649 (C═O), 1587, 1505 (C═C), 1222, 1157 (C−O). ^{1}H NMR (400 MHz, DMSO-d_6) (δ, ppm): 9.93 (*s*, 1H, N−H), 7.67 (*d*, *J* = 8.5 Hz, 2H, Ar−H), 7.62 (*d*, *J* = 8.2 Hz, 1H, Ar−H), 7.53 (*s*, 1H, Ar−H), 7.47 (*d*, *J* = 8.5 Hz, 2H, Ar−H), 7.33 (*s*, 1H, olefinic CH), 7.08 (*d*, *J* = 8.4 Hz, 1H, Ar−H), 4.19 (*q*, *J* = 7.0 Hz, 2H, $O\underline{CH_2}CH_3$), 3.84 (*s*, 3H, OCH_3), 3.82 (*s*, 3H, OCH_3), 1.23 (*t*, *J* = 7.0 Hz, 3H, $OCH_2\underline{CH_3}$). ^{13}C NMR (100 MHz, DMSO-d_6) (δ, ppm): 165.65, 164.94, 151.92, 148.39, 133.81, 132.57, 131.43, 130.61, 128.69, 127.85, 125.38, 121.24, 111.04, 110.95, 60.95, 55.70, 55.60, 14.12. MS (*m*/*z*, %): 389.49 (M^+, 11.10), 254.14 (100). Found: C, 61.47; H, 5.03; N, 3.79; $C_{20}H_{20}ClNO_5$ (389.83) requires C, 61.62; H, 5.17; N, 3.59.

*4.1.3.3. (Z)-Propyl 3-(4-Chlorophenyl)-2-(3,4-dimethoxybenzamido)acrylate (**5c**).* Yield (2.38 g, 59%) mp 155−157 °C. IR (ATR, ν, cm^{-1}): 3324 (NH), 3018 (CH aromatic), 2969, 2937 (CH aliphatic), 1714, 1648 (C═O), 1587, 1505 (C═C), 1275, 1057 (C−O). ^{1}H NMR (400 MHz, DMSO-d_6) (δ, ppm): 9.94 (*s*, 1H, N−H), 7.68 (*d*, *J* = 8.6 Hz, 2H, Ar−H), 7.65−7.59 (*m*, 1H, Ar−H), 7.53 (*d*, *J* = 1.6 Hz, 1H, Ar−H), 7.47 (*d*, *J* = 8.6 Hz, 2H, Ar−H), 7.33 (*s*, 1H, olefinic CH), 7.08 (*d*, *J* = 8.5 Hz, 1H, Ar−H), 4.10 (*t*, *J* = 6.5 Hz, 2H, $O\underline{CH_2}CH_2CH_3$), 3.84 (*s*, 3H, OCH_3), 3.81 (*s*, 3H, OCH_3), 1.61 (*h*, *J* = 7.2 Hz, 2H, $OCH_2\underline{CH_2}CH_3$), 0.88 (*t*, *J* = 7.4 Hz, 3H). ^{13}C NMR (100 MHz, DMSO-d_6) (δ, ppm): 165.76, 165.07, 151.92, 148.39, 133.84, 132.56, 131.48, 130.66, 128.70, 127.89, 125.42, 121.25, 111.05, 110.95, 66.40, 55.69, 55.60, 21.60, 10.32. MS (*m*/*z*,%): 403.67 (M^+, 26.06), 364.77 (100). Found: C, 62.56; H, 5.42; N, 3.59; $C_{21}H_{22}ClNO_5$ (403.86) requires C, 62.45; H, 5.49; N, 3.47.

*4.1.3.4. (Z)-Butyl 3-(4-Chlorophenyl)-2-(3,4-dimethoxybenzamido)acrylate (**5d**).* Yield (1.71 g, 41%) mp 138−140 °C. IR (ATR, ν, cm^{-1}): 3395 (NH), 3018 (CH aromatic), 2874, 2841 (CH aliphatic), 1712, 1649 (C═O), 1587, 1505 (C═C), 1274, 1040 (C−O). ^{1}H NMR (400 MHz, DMSO-d_6) (δ, ppm): 9.97 (*s*, 1H, N−H), 7.67 (*d*, *J* = 8.4 Hz, 2H, Ar−H), 7.63 (*d*, *J* = 7.6 Hz, 1H, Ar−H), 7.55 (*s*, 1H, Ar−H), 7.47 (*d*, *J* = 8.4 Hz, 2H, Ar−H), 7.36 (*s*, 1H, olefinic CH), 7.08 (*d*, *J* = 8.4 Hz, 1H, Ar−H), 4.10 (*t*, *J* = 6.4 Hz, 2H, $O\underline{CH_2}CH_2CH_2CH_3$), 3.84 (*s*, 3H, OCH_3), 3.82 (*s*, 3H, OCH_3), 3.73 (*s*, 2H, $OCH_2\underline{CH_2}CH_2CH_3$), 1.61 (*h*, *J* = 6.8 Hz, 2H, $OCH_2CH_2\underline{CH_2}CH_3$), 0.88 (*t*, *J* = 7.3 Hz, 3H, $OCH_2CH_2CH_2\underline{CH_3}$). ^{13}C NMR (100 MHz, DMSO-d_6) (δ, ppm): 165.57, 165.50, 151.95, 148.39, 133.86, 132.50, 131.45, 130.91, 128.69, 127.50, 125.23, 121.27, 111.04, 110.96, 66.36, 55.70, 55.59, 52.30, 21.57, 10.30. MS (*m*/*z*,%): 417.98 (M^+, 14.52), 304.24 (100). Found: C, 63.11; H, 5.88; N, 3.45; $C_{22}H_{24}ClNO_5$ (417.88) requires C, 63.23; H, 5.79; N, 3.35.

*4.1.3.5. (Z)-Methyl 3-(4-Chlorophenyl)-2-(3,4,5-trimethoxybenzamido)acrylate (**5e**).* Yield (2.46 g, 61%) mp 121−123 °C. IR (ATR, ν, cm^{-1}): 3319 (NH), 2998, 2939, 2874 (CH aliphatic), 1707, 1658 (C═O), 1586, 1505 (C═C), 1209, 1176 (C−O). ^{1}H NMR (400 MHz, DMSO-d_6) (δ, ppm): 10.08 (*s*, 1H, N−H), 7.69 (*d*, *J* = 8.4 Hz, 2H, Ar−H), 7.50 (*d*, *J* = 8.4 Hz, 2H, Ar−H), 7.39 (*s*, 1H, olefinic CH), 7.34 (*s*, 2H, Ar−H), 3.86 (*s*, 6H, $2OCH_3$), 3.75 (*s*, 6H, $2OCH_3$). ^{13}C NMR (100 MHz, DMSO-d_6) (δ, ppm): 165.90, 165.85, 153.20, 141.13, 134.44, 132.86, 131.98, 131.51, 129.24, 128.49, 127.76, 105.84, 60.57, 56.54, 52.82. MS (*m*/*z*, %): 405.23 (M^+,

https://doi.org/10.1021/acsomega.3c05051
ACS Omega 2023, 8, 38394−38405

15.02), 44.95 (100). Found C, 59.32; H, 5.07; N, 3.36; $C_{20}H_{20}ClNO_6$ (405.83) requires C, 59.19; H, 4.97; N, 3.45.

*4.1.3.6. (Z)-Ethyl 3-(4-Chlorophenyl)-2-(3,4,5-trimethoxybenzamido)acrylate (**5f**).* Yield (2.44 g, 58%) mp 159−161 °C. IR (ATR, ν, cm^{-1}): 3236 (NH), 3010 (CH aromatic), 2961, 2838 (CH aliphatic), 1716, 1630 (C═O), 1597, 1508 (C═C), 1283, 1194 (C−O). ^{1}H NMR (400 MHz, DMSO-d_6) (δ, ppm): 10.04 (*s*, 1H, N−H), 7.69 (*d*, *J* = 8.6 Hz, 2H, Ar−H), 7.50 (*d*, *J* = 8.6 Hz, 2H, Ar−H), 7.37 (*s*, 1H, olefinic CH), 7.32 (*s*, 2H, Ar−H), 4.21 (*q*, *J* = 7.1 Hz, 2H, OCH_2CH_3), 3.85 (*s*, 6H, $2OCH_3$), 3.75 (*s*, 3H, OCH_3), 1.25 (*t*, *J* = 7.1 Hz, 3H, OCH_2CH_3). ^{13}C NMR (100 MHz, DMSO-d_6) (δ, ppm): 165.94, 165.27, 153.19, 141.08, 134.37, 132.92, 131.94, 131.23, 129.22, 128.65, 128.03, 105.79, 61.47, 60.57, 56.54, 14.60. MS (*m*/*z*, %): 419.46 (M^+, 8.53), 213.18 (100). Found: C, 59.88; H, 5.40; N, 3.22; $C_{21}H_{22}ClNO_6$ (419.86) requires C, 60.07; H, 5.28; N, 3.34.

*4.1.3.7. (Z)-Propyl 3-(4-Chlorophenyl)-2-(3,4,5-trimethoxybenzamido)acrylate (**5g**).* Yield (2.34 g, 54%) mp 152−154 °C. IR (ATR, ν, cm^{-1}): 3322 (NH), 2971, 2841 (CH aliphatic), 1707, 1658 (C═O), 1586, 1511 (C═C), 1285, 1209 (C−O). ^{1}H NMR (400 MHz, DMSO-d_6) (δ, ppm): 10.05 (*s*, 1H, N−H), 7.70 (*d*, *J* = 8.5 Hz, 2H, Ar−H), 7.50 (*d*, *J* = 8.5 Hz, 2H, Ar−H), 7.37 (*s*, 1H, olefinic CH), 7.32 (*s*, 2H, Ar−H), 4.12 (*t*, *J* = 6.5 Hz, 2H, $O\underline{CH_2}CH_2CH_3$), 3.85 (*s*, 6H, $2OCH_3$), 3.75 (*s*, 3H, OCH_3), 1.63 (*q*, *J* = 6.9 Hz, 2H, $OCH_2\underline{CH_2}CH_3$), 0.91 (*t*, *J* = 7.4 Hz, 3H, $OCH_2CH_2\underline{CH_3}$). ^{13}C NMR (100 MHz, DMSO-d_6) (δ, ppm): 166.04, 165.37, 153.18, 141.05, 134.38, 132.89, 131.97, 131.29, 129.21, 128.70, 128.09, 105.77, 66.89, 60.57, 56.53, 22.05, 10.77. MS (*m*/*z*, %): 433.62 (M^+, 12.12), 264.25 (100). Found: C, 61.04; H, 5.47; N, 3.05; $C_{22}H_{24}ClNO_6$ (433.88) requires C, 60.90; H, 5.58; N, 3.23.

*4.1.3.8. (Z)-Isopropyl 3-(4-Chlorophenyl)-2-(3,4,5-trimethoxybenzamido)acrylate (**5h**).* Yield (2.69 g, 62%) mp 126−128 °C. IR (ATR, ν, cm^{-1}): 3283 (NH), 2940, 2875 (CH aliphatic), 1707, 1658 (C═O), 1586, 1513 (C═C), 1304, 1079 (C−O). ^{1}H NMR (400 MHz, DMSO-d_6) (δ, ppm): 10.01 (*s*, 1H, N−H), 7.68 (*d*, *J* = 8.6 Hz, 2H, Ar−H), 7.49 (*d*, *J* = 8.6 Hz, 2H, Ar−H), 7.32 (*s*, 1H, olefinic CH), 7.31 (*s*, 2H, Ar−H), 5.00 (*p*, *J* = 6.2 Hz, 1H, $O\underline{CH}(CH_3)_2$), 3.85 (*s*, 6H, $2OCH_3$), 3.74 (*s*, 3H, OCH_3), 1.25 (*d*, *J* = 6.2 Hz, 6H, $OCH(\underline{CH_3})_2$). ^{13}C NMR (100 MHz, DMSO-d_6) (δ, ppm): 165.99, 164.78, 153.18, 141.03, 134.28, 132.96, 131.91, 130.84, 129.20, 128.78, 128.45, 105.76, 69.01, 60.57, 56.54, 22.06. MS (*m*/*z*, %): 433.78 (M^+, 18.84), 101.98 (100). Found: C, 60.96; H, 5.64; N, 3.11; $C_{22}H_{24}ClNO_6$ (433.88) requires C, 60.90; H, 5.58; N, 3.23.

*4.1.3.9. (Z)-Butyl 3-(4-Chlorophenyl)-2-(3,4,5-trimethoxybenzamido)acrylate (**5i**).* Yield (2.37 g, 53%) mp 118−120 °C. IR (ATR, ν, cm^{-1}): 3222 (NH), 3082, 3001 (CH aromatic), 2958, 2939 (CH aliphatic), 1714, 1627 (C═O), 1598, 1524 (C═C), 1297, 1191 (C−O). ^{1}H NMR (400 MHz, DMSO-d_6) (δ, ppm): 10.05 (*d*, *J* = 10.6 Hz, 1H, N−H), 7.68 (*d*, *J* = 8.5 Hz, 2H, Ar−H), 7.49 (*d*, *J* = 8.5 Hz, 2H, Ar−H), 7.37 (*d*, *J* = 6.9 Hz, 1H, olefinic CH), 7.32 (*d*, *J* = 7.5 Hz, 2H, Ar−H), 4.11 (*t*, *J* = 6.5 Hz, 2H, $O\underline{CH_2}CH_2CH_2CH_3$), 3.85 (*s*, 6H, $2OCH_3$), 3.74 (*s*, 5H, OCH_3 and $OCH_2\underline{CH_2}CH_2CH_3$), 1.63 (*dt*, *J* = 13.9, 6.9 Hz, 2H, $OCH_2CH_2\underline{CH_2}CH_3$), 0.90 (*t*, *J* = 7.4 Hz, 3H, $OCH_2CH_2CH_2\underline{CH_3}$). ^{13}C NMR (100 MHz, DMSO-d_6) (δ, ppm): 165.47, 165.41, 152.74, 140.70, 134.01, 132.41, 131.52, 131.07, 128.76, 128.07, 127.32, 105.40, 66.45, 60.10, 56.07, 52.34, 21.61, 10.30. MS (*m*/*z*, %): 447.95 (M^+, 23.86), 75.92 (100). Found: C, 61.84; H, 6.07; N, 2.94; $C_{23}H_{26}ClNO_6$ (447.91) requires C, 61.67; H, 5.85; N, 3.13.

4.2. Biological studies. *4.2.1. In Vitro Cytotoxicity Assay.* MTT assay (IC_{50}, μM) was performed in accordance with the previously reported method.[15] See Supporting Information Appendix A.

4.2.2. Tubulin Assay. The β-tubulin inhibitory activity of the test compounds was assessed according to the manufacturer's instructions. See Supporting Information Appendix A.

4.2.3. Cell Cycle Study. The cell cycle study of test compound **4b** against MDA-MB-231 cancerous cells was carried out in accordance with the manufacturer's instructions. See Supporting Information Appendix A.

4.2.4. Cell Apoptosis Study. Cell apoptosis assay of the test compound **4b** against MDA-MB-231 cells was carried out in accordance with the manufacturer's instructions. See Supporting Information Appendix A.

4.2.5. In Vivo Antitumor Screening. For the in vivo studies, the acrylic acid derivative **4b** was converted into sodium salt to enhance the bioavailability. See Supporting Information Appendix A.

4.2.6. Molecular Docking Study. See Supporting Information Appendix A.

■ ASSOCIATED CONTENT

Supporting Information

The Supporting Information is available free of charge at https://pubs.acs.org/doi/10.1021/acsomega.3c05051.

All the spectral analysis such as IR, ^{1}H NMR, ^{13}C NMR, and MS spectra for all prepared compounds and detailed descriptions (PDF)

■ AUTHOR INFORMATION

Corresponding Author

Islam Zaki − *Pharmaceutical Organic Chemistry Department, Faculty of Pharmacy, Port Said University, Port Said 42526, Egypt*; orcid.org/0000-0002-2026-7373; Email: Eslam.Zaki@pharm.psu.edu.eg

Authors

Eman Fayad − *Department of Biotechnology, College of Sciences, Taif University, Taif 21944, Saudi Arabia*

Sarah Awwadh Altalhi − *Department of Biotechnology, College of Sciences, Taif University, Taif 21944, Saudi Arabia*

Matokah M. Abualnaja − *Department of Chemistry, Faculty of Applied Science, Umm Al-Qura University, Makkah Al Mukarrama 24230, Saudi Arabia*

Abdulmohsen H. Alrohaimi − *Department of Pharmacy Practice, College of Pharmacy, Shaqra University, Shaqra 11961, Saudi Arabia*

Fahmy G. Elsaid − *Biology Department, College of Science, King Khalid University, Asir, Abha 61421, Saudi Arabia*

Ali H. Abu Almaaty − *Zoology Department, Faculty of Science Port Said University, Port Said 42526, Egypt*

Rasha Mohammed Saleem − *Department of Laboratory Medicine, Faculty of Applied Medical Sciences, Al-Baha University, Al-Baha 65431, Saudi Arabia*

https://doi.org/10.1021/acsomega.3c05051
ACS Omega 2023, 8, 38394−38405

Mohammed A. Bazuhair − *Department of Clinical Pharmacology, Faculty of Medicine, King Abdulaziz University, Jeddah 21589, Saudi Arabia*

Ali Hassan Ahmed Maghrabi − *Department of Biology, Faculty of Applied Science, Umm Al-Qura University, Makkah 24381, Saudi Arabia*

Botros Y. Beshay − *Pharmaceutical Sciences (Pharmaceutical Chemistry) Department, College of Pharmacy, Arab Academy for Science, Technology and Maritime Transport, Alexandria 21913, Egypt*

Complete contact information is available at: https://pubs.acs.org/10.1021/acsomega.3c05051

Funding

The authors extend their appreciation to the Deanship of Scientific Research at King Khalid University for funding this work through large group Research project under grant number RGP2/12/44.

Notes

The authors declare no competing financial interest.

■ ACKNOWLEDGMENTS

The authors extend their appreciation to the Deanship of Scientific Research at King Khalid University for funding this work through large group Research project under grant number RGP2/12/44.

■ REFERENCES

(1) Siegel, R. L.; Miller, K. D.; Wagle, N. S.; Jemal, A. Cancer statistics, 2023. *Ca-Cancer J. Clin.* **2023**, *73*, 17−48.

(2) Truty, M. J.; Kendrick, M. L.; Nagorney, D. M.; Smoot, R. L.; Cleary, S. P.; Graham, R. P.; Goenka, A. H.; Hallemeier, C. L.; Haddock, M. G.; Harmsen, W. S.; et al. Factors predicting response, perioperative outcomes, and survival following total neoadjuvant therapy for borderline/locally advanced pancreatic cancer. *Ann. Surg.* **2021**, *273*, 341−349.

(3) Adams, E.; Wildiers, H.; Neven, P.; Punie, K. Sacituzumab govitecan and trastuzumab deruxtecan: two new antibody-drug conjugates in the breast cancer treatment landscape. *ESMO Open* **2021**, *6*, 100204.

(4) Akhmanova, A.; Kapitein, L. C. Mechanisms of microtubule organization in differentiated animal cells. *Nat. Rev. Mol. Cell Biol.* **2022**, *23*, 541−558.

(5) Yuki, R.; Ikeda, Y.; Yasutake, R.; Saito, Y.; Nakayama, Y. SH2D4A promotes centrosome maturation to support spindle microtubule formation and mitotic progression. *Sci. Rep.* **2023**, *13*, 2067.

(6) Mascanzoni, F.; Iannitti, R.; Colanzi, A. Functional Coordination among the Golgi Complex, the Centrosome and the Microtubule Cytoskeleton during the Cell Cycle. *Cells* **2022**, *11*, 354.

(7) Valdez, V. A.; Neahring, L.; Petry, S.; Dumont, S. Mechanisms underlying spindle assembly and robustness. *Nat. Rev. Mol. Cell Biol.* **2023**, *24*, 523−542.

(8) Barbolina, M. V. Targeting Microtubule-Associated Protein Tau in Chemotherapy-Resistant Models of High-Grade Serous Ovarian Carcinoma. *Cancers* **2022**, *14*, 4535.

(9) Iacopetta, D.; Ceramella, J.; Baldino, N.; Sinicropi, M. S.; Catalano, A. Targeting Breast Cancer: An Overlook on Current Strategies. *Int. J. Mol. Sci.* **2023**, *24*, 3643.

(10) Baytas, S. N. Recent Advances in Combretastatin A-4 Inspired Inhibitors of Tubulin Polymerization: An Update. *Curr. Med. Chem.* **2022**, *29*, 3557−3585.

(11) Zaki, I.; Moustafa, A. M. Y.; Beshay, B. Y.; Masoud, R. E.; Elbastawesy, M. A. I.; Abourehab, M. A. S.; Zakaria, M. Y. Design and synthesis of new trimethoxylphenyl-linked combretastatin analogues loaded on diamond nanoparticles as a panel for ameliorated solubility and antiproliferative activity. *J. Enzyme Inhib. Med. Chem.* **2022**, *37*, 2679−2701.

(12) Al-Warhi, T.; Alqahtani, L. S.; Alsharif, G.; Abualnaja, M.; Abu Ali, O. A.; Qahl, S. H.; Althagafi, H. A. E.; Alharthi, F.; Jafri, I.; Elsaid, F. G.; et al. Design, Synthesis, and Investigation of Cytotoxic Activity of cis-Vinylamide-Linked Combretastatin Analogues as Potential Anticancer Agents. *Symmetry* **2022**, *14*, 2088.

(13) Mustafa, M.; A Mostafa, Y.; Elbaky, A.; Mohamed, M.; Abdelhamid, D.; Abdelhafez, E.; Aly, O. M. Combretastatin A-4 analogs: Past, present, and future directions. *Octahedron Drug Res.* **2022**, *1*, 55−64.

(14) Bukhari, S. N. A.; Zakaria, M. Y.; Munir, M. U.; Ahmad, N.; Elsherif, M. A.; Badr, R. E.; Hassan, A. K.; Almaaty, A. H. A.; Zaki, I. Design, Synthesis, In Vitro Biological Activity Evaluation and Stabilized Nanostructured Lipid Carrier Formulation of Newly Synthesized Schiff Bases-Based TMP Moieties. *Pharmaceuticals* **2022**, *15*, 679.

(15) Mohamed, K. O.; Zaki, I.; El-Deen, I. M.; Abdelhameid, M. K. A new class of diamide scaffold: Design, synthesis and biological evaluation as potent antimitotic agents, tubulin polymerization inhibition and apoptosis inducing activity studies. *Bioorg. Chem.* **2019**, *84*, 399−409.

(16) Dhiman, A.; Sharma, R.; Singh, R. K. Target-based anticancer indole derivatives and insight into structure-activity relationship: A mechanistic review update (2018−2021). *Acta Pharm. Sin.* **2022**, *12*, 3006−3027.

(17) Ebenezer, O.; Shapi, M.; Tuszynski, J. A. A Review of the Recent Developments of Molecular Hybrids Targeting Tubulin Polymerization. *Int. J. Mol. Sci.* **2022**, *23*, 4001.

(18) Wang, C.; Zhang, Y.; Xing, D. Emerging Tubulin Inhibitors: A New Hope for Fungicides. *J. Agric. Food Chem.* **2021**, *69*, 11151−11153.

(19) Zhao, R.; Wu, Y.; Zhang, Y.; Ling, J.; Liu, X.; Xiang, J.; Zeng, X.; Chen, T. Designing anticancer combretastatin A-4 analogues with aggregation-induced emission characteristics. *Sci. China Chem.* **2022**, *65*, 694−698.

(20) Weng, H.; Li, J.; Zhu, H.; Carver Wong, K. F.; Zhu, Z.; Xu, J. An update on the recent advances and discovery of novel tubulin colchicine binding inhibitors. *Future Med. Chem.* **2023**, *15*, 73−95.

(21) Asl, M. H.; Khelejani, F. P.; Mahdavi, S. Z. B.; Emrahi, L.; Jebelli, A.; Mokhtarzadeh, A. The various regulatory functions of long noncoding RNAs in apoptosis, cell cycle, and cellular senescence. *J. Cell. Biochem.* **2022**, *123*, 995−1024.

(22) Kaloni, D.; Diepstraten, S. T.; Strasser, A.; Kelly, G. L. BCL-2 protein family: attractive targets for cancer therapy. *Apoptosis* **2023**, *28*, 20−38.

(23) Koren, E.; Fuchs, Y. Modes of Regulated Cell Death in Cancer. *Cancer Discov.* **2021**, *11*, 245−265.

(24) Al-Warhi, T.; Abualnaja, M.; Ali, O. A. A.; Althobaiti, F.; Alharthi, F.; Elsaid, F. G.; Shati, A. A.; Fayad, E.; Elghareeb, D.; Almaaty, A. H. A.; et al. Synthesis and Biological Activity Screening of Newly Synthesized Trimethoxyphenyl-Based Analogues as Potential Anticancer Agents. *Molecules* **2022**, *27*, 4621.

(25) Zaki, I.; Masoud, R. E.; Hamoud, M. M. S.; Ali, O. A. A.; Abualnaja, M.; Fayad, E.; Almaaty, A. H. A.; Elnaghia, L. K. Design, synthesis and cytotoxicity screening of new synthesized pyrimidine-5-carbonitrile derivatives showing marked apoptotic effect. *J. Mol. Struct.* **2022**, *1259*, 132749.

(26) Al-Warhi, T.; Alqahtani, L. S.; Abualnaja, M.; Beigh, S.; Ali, O. A. A.; Elsaid, F. G.; Shati, A. A.; Saleem, R. M.; Maghrabi, A. H. A.; Alharthi, A. A.; et al. Design, Synthesis, and In Vitro Antiproliferative Screening of New Hydrazone Derivatives Containing cis-(4-Chlorostyryl) Amide Moiety. *Symmetry* **2022**, *14*, 2457.

(27) Yang, F.; Hu, Z.; Guo, Z. Small-Molecule Inhibitors Targeting FEN1 for Cancer Therapy. *Biomolecules* **2022**, *12*, 1007.

(28) Zhang, S.; Liu, H.; Yang, N.; Xiong, L.; Wang, B. Synthesis and evaluation of novel xanthine-acrylamides and xanthine-acrylates as insecticidal agents. *Pest Manage. Sci.* **2022**, *78*, 2086−2095.

(29) Radwan, R. R.; Ali, H. E. Radiation-synthesis of chitosan/poly (acrylic acid) nanogel for improving the antitumor potential of rutin in hepatocellular carcinoma. *Drug Delivery Transl. Res.* **2021**, *11*, 261−278.
(30) Du, S.; Meng, F.; Duan, W.; Liu, Q.; Li, H.; Peng, X. Oxidative stress responses in two marine diatoms during acute n-butyl acrylate exposure and the toxicological evaluation with the IBRv2 index. *Ecotoxicol. Environ. Saf.* **2022**, *240*, 113686.
(31) Xie, Y.; Liu, Y.; Sun, J.; Zheng, L. Synthesis of mitochondria-targeted ferulic acid amide derivatives with antioxidant, anti-inflammatory activities and inducing mitophagy. *Bioorg. Chem.* **2022**, *127*, 106037.
(32) Sun, W.-X.; Han, H.-W.; Yang, M.-K.; Wen, Z.-L.; Wang, Y.-S.; Fu, J.-Y.; Lu, Y.-T.; Wang, M.-Y.; Bao, J.-X.; Lu, G.-H.; et al. Design, synthesis and biological evaluation of benzoylacrylic acid shikonin ester derivatives as irreversible dual inhibitors of tubulin and EGFR. *Bioorg. Med. Chem.* **2019**, *27*, 115153.
(33) Hao, M.; Guo, Y.; Zhang, Z.; Zhou, H.; Gu, Q.; Xu, J. 6-acrylic phenethyl ester-2-pyranone derivative induces apoptosis and G2/M arrest by targeting GRP94 in colorectal cancer. *Bioorg. Chem.* **2022**, *123*, 105802.
(34) Bommagani, S.; Ponder, J.; Penthala, N. R.; Janganati, V.; Jordan, C. T.; Borrelli, M. J.; Crooks, P. A. Indole carboxylic acid esters of melampomagnolide B are potent anticancer agents against both hematological and solid tumor cells. *Eur. J. Med. Chem.* **2017**, *136*, 393−405.
(35) Vineethakumari, C.; Lüders, J. Microtubule Anchoring: Attaching Dynamic Polymers to Cellular Structures. *Front. Cell Dev. Biol.* **2022**, *10*, 867−870.
(36) Yuan, X.-Y.; Song, C.-H.; Liu, X.-J.; Wang, X.; Jia, M.-Q.; Wang, W.; Liu, W.-B.; Fu, X.-J.; Jin, C.-Y.; Song, J.; et al. Discovery of novel N-benzylarylamide-dithiocarbamate based derivatives as dual inhibitors of tubulin polymerization and LSD1 that inhibit gastric cancers. *Eur. J. Med. Chem.* **2023**, *252*, 115281.
(37) Pandey, K.; Katuwal, N. B.; Park, N.; Hur, J.; Cho, Y. B.; Kim, S. K.; Lee, S. A.; Kim, I.; Lee, S.-R.; Moon, Y. W. Combination of Abemaciclib following Eribulin Overcomes Palbociclib-Resistant Breast Cancer by Inhibiting the G2/M Cell Cycle Phase. *Cancers* **2022**, *14*, 210.
(38) Liu, R.; Huang, M.; Zhang, S.; Li, L.; Li, M.; Sun, J.; Wu, L.; Guan, Q.; Zhang, W. Design, synthesis and bioevaluation of 6-aryl-1-(3,4,5-trimethoxyphenyl)-1H-benzo[d]imidazoles as tubulin polymerization inhibitors. *Eur. J. Med. Chem.* **2021**, *226*, 113826.
(39) El-Lateef, H. M. A.; Elmaaty, A. A.; Ghany, L. M. A. A.; Abdel-Aziz, M. S.; Zaki, I.; Ryad, N. Design and Synthesis of 2-(4-Bromophenyl)Quinoline-4-Carbohydrazide Derivatives via Molecular Hybridization as Novel Microbial DNA-Gyrase Inhibitors. *ACS Omega* **2023**, *8*, 17948−17965.
(40) Abdelhameid, M. K.; Zaki, I.; Mohammed, M. R.; Mohamed, K. O. Design, synthesis, and cytotoxic screening of novel azole derivatives on hepatocellular carcinoma (HepG2 Cells). *Bioorg. Chem.* **2020**, *101*, 103995.
(41) Duan, Y.-T.; Man, R.-J.; Tang, D.-J.; Yao, Y.-F.; Tao, X.-X.; Yu, C.; Liang, X.-Y.; Makawana, J. A.; Zou, M.-J.; Wang, Z.-C.; et al. Design, Synthesis and Antitumor Activity of Novel link-bridge and B-Ring Modified Combretastatin A-4 (CA-4) Analogues as Potent Antitubulin Agents. *Sci. Rep.* **2016**, *6*, 25387.
(42) BIOVIA, Discovery Studio. *Molecular Modeling and Simulation, [4.5]*; Dassault Systemes: San Diego, 2019.

https://doi.org/10.1021/acsomega.3c05051
ACS Omega 2023, 8, 38394−38405